

Figure 1. Central derivatives (red lines) used for the inversion and number of data-points every 5 kyrs from Ref.1 (a) and Ref.2 (b) (Methods).

Model parameter	Min	Max
$t [ka]$	-797,099.0	0.0
$\gamma \left[\frac{ppmv}{yr} \right]$	0.0	0.08
$\beta \left[\frac{ppmv}{yr \text{ } ^\circ C} \right]$	0.0	0.008
k	1	100
ω	-1.0	3.0

Table I. Range values for uniform sampling of t , γ , β , k and ω used for the inversion. k and ω are dimensionless quantities.

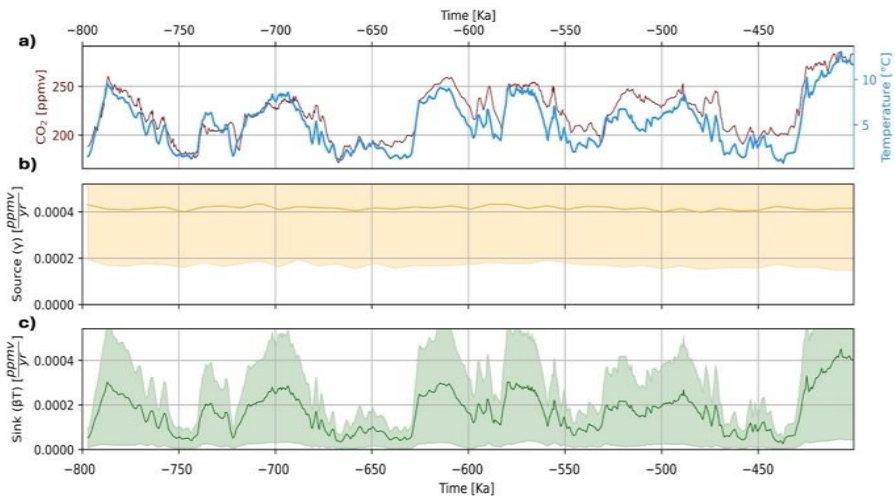


Figure 2. Results from the first test as a simple McMC inversion. (a) 800-400 ka subset including the atmospheric CO_2 and T reconstructions from Refs. 1, 3 shown for reference with flux results. (b) γ source flux time history. (c) βT sink flux time history. The reduced variability and magnitude align with results from the main text over this period.

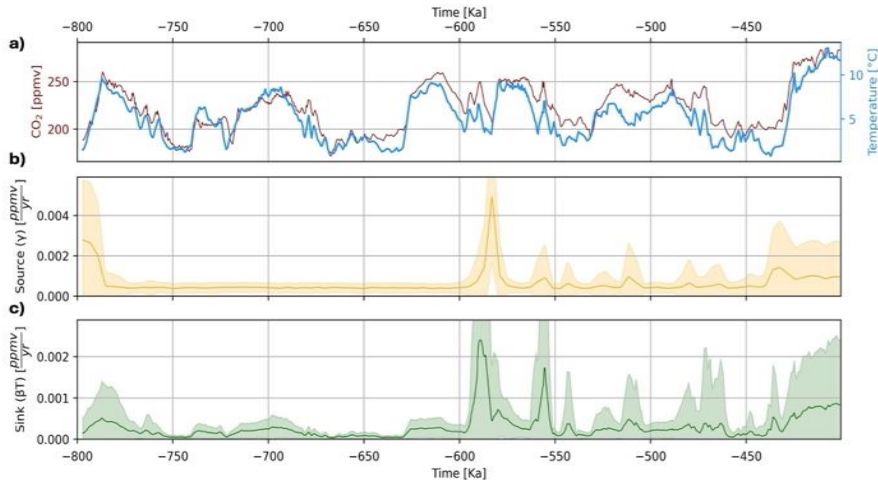


Figure 3. Results from the second test as a rj-McMC inversion. (a) 800-400 ka subset including the atmospheric CO_2 and T reconstructions from Refs. 1, 3 shown for reference with flux results. (b) γ source flux time history. (c) βT sink flux time history. The higher variability compared to the first test arises from the use of a rj-McMC, where the small γ and βT magnitudes align with reduced pre-400 ka flux variability in the main text.

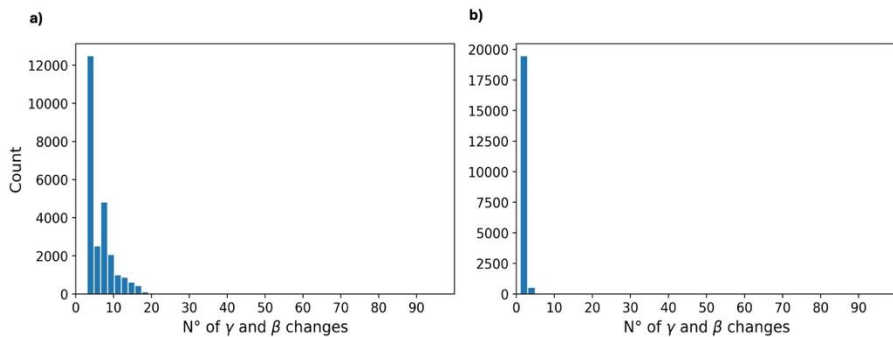


Figure 4. Distribution for the number of γ and βT changes from the main analysis (a) and the inversion from the second test (b). Although results from the second test express pre-400 ka variability, the number of γ and βT changes is lower (i.e., ~1), confirming the reduce flux variability pre-400 ka.

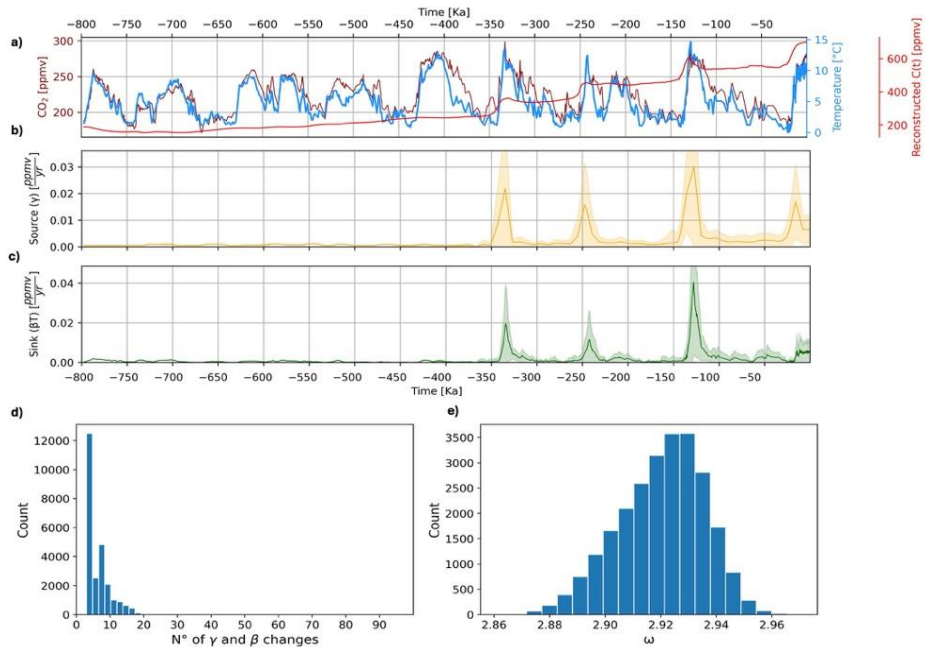


Figure 5. Results from the main text inversion as a comparable reference with results from test in Fig.5. (a) CO₂, T, and reconstructed C(t) curve using the retrieved γ and βT fluxes. **(b-c)** Retrieved γ and βT flux time series. **(d)** Distribution for the number of γ and βT changes. **(e)** The distribution of the uncertainty scaling parameter ω . The high uncertainty on inverted data leads to high value of ω and reduced variability of fluxes.

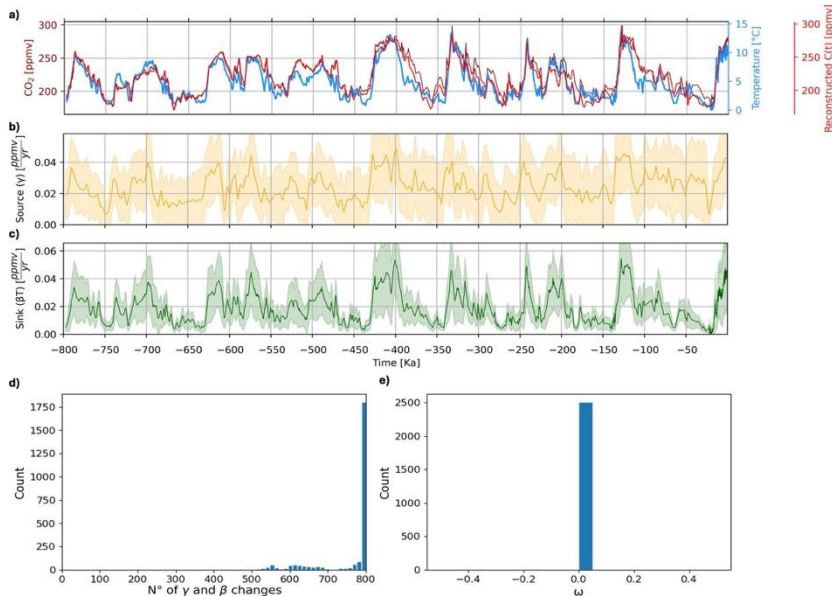


Figure 6. Results from the inversion when setting $\omega=0$. (a) CO_2 , T , and reconstructed $C(t)$ curve using the retrieved γ and βT fluxes. (b-c) Retrieved γ and βT fluxes time histories. (d) Distribution for the number of γ and βT changes. (e) The distribution of the uncertainty scaling parameter ω . The use of no scaling factor ω leads to a large increment in the number of γ and βT changes, preventing to assess significant carbon cycle flux changes.

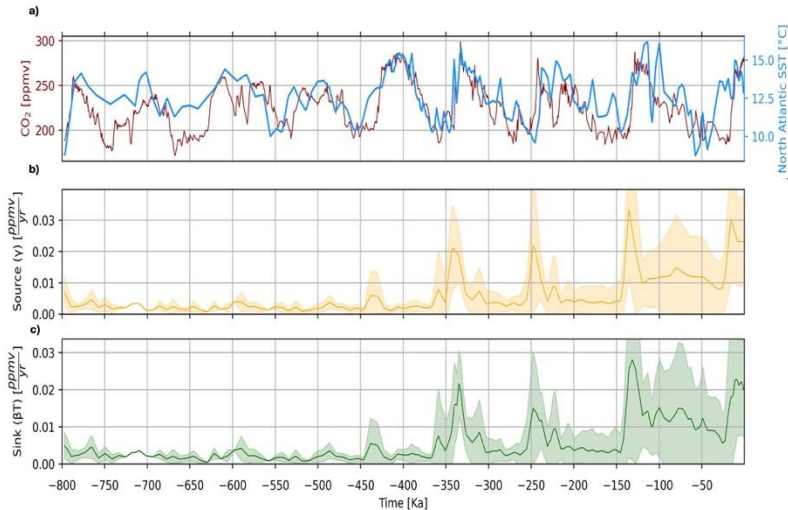


Figure 7. Flux histories reconstruction using the global CO_2 record and the alkenone SST reconstruction in the North Atlantic from main text Refs. 1, and 10, respectively. (a) Global CO_2 and local North Atlantic SST record. (b) Source flux time history reconstruction. (c) Sink flux time history.

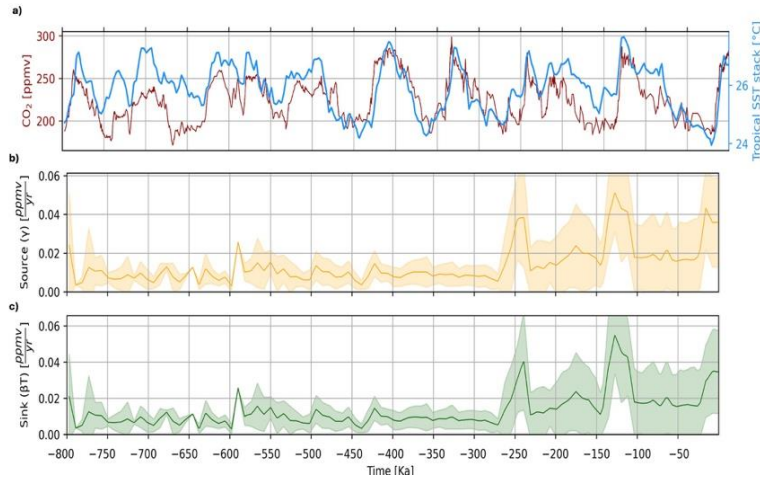


Figure 8. Flux histories reconstruction using the global CO_2 record and the stacked alkenone SST reconstruction at the tropics from main text Refs. 1, and 11, respectively. (a) Global CO_2 and tropical stack SST record. (b) Source flux time history reconstruction. (c) Sink flux time history.

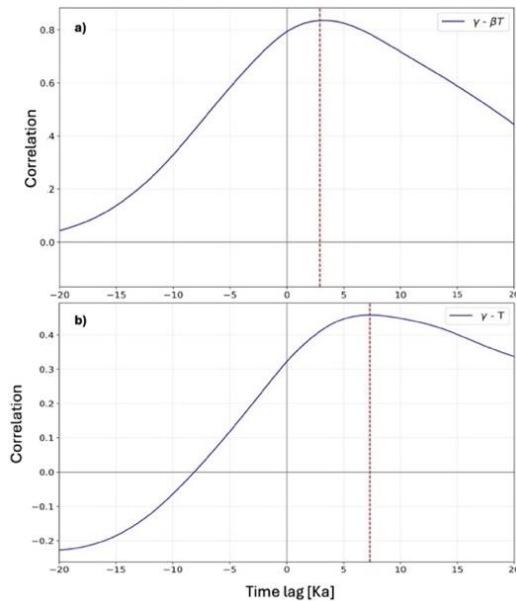


Figure 9. Cross-correlation analysis of γ against βT (a) and T (b). Maximum lag correlation is found with a lag of ~ 3 ka and ~ 7 ka.